Bi-allelic LoF *NRROS* Variants Impairing Active TGF-β1 Delivery Cause a Severe Infantile-Onset Neuro degenerative Condition with Intracranial Calcification

Xiaomin Dong,[1,2,10] Natalie B. Tan,[1,2,3,10] Katherine B. Howell,[1,2,4] Sabina Barresi,[5] Jeremy L. Freeman,[1,4] Davide Vecchio,[5] Maria Piccione,[6] Francesca Clementina Radio,[5] Daniel Calame,[7,8] Shan Zong,[1] Stefanie Eggers,[1,3] Ingrid E. Scheffer,[1,2,4,9] Tiong Y. Tan,[1,2,3] Nicole J. Van Bergen,[1,2] Marco Tartaglia,[5] John Christodoulou,[1,2,3,*] and Susan M. White[1,2,3,*]

Negative regulator of reactive oxygen species (NRROS) is a leucine-rich repeat-containing protein that uniquely associates with latent transforming growth factor beta-1 (TGF- β1) and anchors it on the cell surface; this anchoring is required for activation of TGF-β1 in macrophages and microglia. We report six individuals from four families with bi-allelic variants in *NRROS*. All affected individuals had neurodegenerative disease with refractory epilepsy, developmental regression, and reduced white matter volume with delayed myelination. The clinical course in affected individuals began with normal development or mild developmental delay, and the onset of seizures occurred within the first year of life, followed by developmental regression. Intracranial calcification was detected in three individuals. The phenotypic features in affected individuals are consistent with those observed in the *Nrros* knockout mouse, and they overlap with those seen in the human condition associated with TGF-β1 deficiency. The disease-causing *NRROS* variants involve two significant functional NRROS domains. These variants result in aberrant NRROS proteins with impaired ability to anchor latent TGF-β1 on the cell surface. Using confocal microscopy in HEK293T cells, we demonstrate that wild-type and mutant NRROS proteins co-localize with latent TGF-β1 intracellularly. However, using flow cytometry, we show that our mutant NRROS proteins fail to anchor latent TGF-β1 at the cell surface in comparison to wild-type NRROS. Moreover, wild-type NRROS rescues the defect of our disease-associated mutants in presenting latent TGF-β1 to the cell surface. Taken together, our findings suggest that loss of NRROS function causes a severe childhood-onset neurodegenerative condition with features suggestive of a disordered response to inflammation.

NRROS (MIM: 615322) encodes a transmembrane protein with leucine-rich repeat domains that influence transforming growth factor beta-1 (TGF-β1) signaling and other proteins associated with innate immunity.[1,2] As a negative regulator, negative regulator of reactive oxygen species (NRROS) has been found to inhibit reactive oxygen species (ROS) production.[3,4] NRROS is also implicated in osteoclast and neural cell differentiation during development, with reports of an essential role in microglial development.[4,5] TGF-β1 is encoded by the gene *TGFB1* (MIM: 190180) and initially processed as biologically inactive latent TGF-β1, and the release of active TGF-β1 is dependent upon binding partners of latent TGF-β1.[2] NRROS has recently been identified as a novel binding partner of latent TGF-β1.[2] The specific binding of NRROS with latent TGF-β1 releases active TGF-β1 for the activation of TGF-β signaling in myeloid leukemia cells and THP-1 monocytes.[2,6] Activation of TGF-β1 is essential in the central nervous system (CNS).[2] Increased neural cell death and microgliosis have been observed in mice deficient in TGF-β1.[7] Similarly, *Nrros* knockout mice develop paraparesis with demyelination, with noted loss of microglia and axons.[2] The underlying cause of abnormalities in *Nrros* knockout mice is thought to be reduced activation of TGF-β1 in microglia. Therefore, these observations suggest that the TGF-β signaling pathway plays an important role in CNS development, and that aberrant NRROS function could be detrimental to neuronal function.[2,7,8]

We report six individuals from four families with rare bi-allelic germline variants in the *NRROS* gene (Table 1 and Supplemental Notes). Development in the first year of life ranged from normal to moderate global developmental delay. All affected individuals were hypotonic early in life, and five later developed hypertonia that was predominantly peripheral. All had seizure onset before age one year, and the first seizure type included febrile seizures, infantile spasms, focal seizures, and myoclonic seizures. All had a severe and progressive developmental regression following seizure onset. Seizures were refractory to multiple antiseizure medications in all, and typically occurred at frequencies of multiple seizures daily or multiple seizures hourly. Five affected individuals have encountered problems with recurrent aspiration, and all have required enteral feeding. The older children in this cohort (II:3 in Family 3, II:2 in Family 4) require

[1]Murdoch Children's Research Institute, Parkville, Victoria 3052, Australia; [2]Department of Paediatrics, University of Melbourne, Parkville, Victoria 3052, Australia; [3]Victorian Clinical Genetics Services, Parkville, Victoria 3052, Australia; [4]Department of Neurology, Royal Children's Hospital, Parkville, Victoria 3052, Australia; [5]Genetics and Rare Diseases Research Division, Ospedale Pediatrico Bambino Gesù, Rome 00146, Italy; [6]Department of Science for Health Promotion and Mother and Child Care, Università degli Studi di Palermo, Palermo 90127, Italy; [7]Baylor College of Medicine, Houston, TX 77030, USA; [8]Texas Children's Hospital, Houston, TX 77030, USA; [9]Department of Medicine, University of Melbourne, Austin Health, Heidelberg, Victoria 3084, Australia
[10]These authors contributed equally to this work
*Correspondence: john.christodoulou@mcri.edu.au (J.C.), sue.white@vcgs.org.au (S.M.W.)
https://doi.org/10.1016/j.ajhg.2020.02.014.

Table 1. Clinical Features and *NRROS* Variants of Affected Individuals

Family	**1**	**1**	**1**	**2**	**3**	**4**
Pedigree ID	**II:2**	**II:3**	**II:4**	**II:2**	**II:3**	**II:2**
Gene Variant						
NRROS, g. (GRCh37/hg19)	chr3:196388493GC > G, homozygous	chr3:196388493GC > G, homozygous	chr3:196388493GC > G, homozygous	chr3:196388493GC > G, homozygous	chr3:196388157TG > T, homozygous	variant 1 (paternal): chr3:196388701AC > A variant 2 (maternal): chr3:196381439T > C
NRROS, c. (RefSeq NM_198565.1)	c.1981delC	c.1981delC	c.1981delC	c.1981delC	c.1644delG	variant 1: c.190delC variant 2: c.29T > C
NRROS, p. (RefSeq NP_940967.1)	p.Leu661Serfs*97	p.Leu661Serfs*97	p.Leu661Serfs*97	p.Leu661Serfs*97	p.Thr549Profs*82	variant 1: p.Leu64Trpfs*81 variant 2: p.Leu10Pro
Age at onset of symptoms	7 months	10 months	9 months	birth	12 months	6 months
Age at death	4 years and 2 months	3 years and 3 months	still alive at 20 months	2 years and 2 months	still alive at 9 years and 3 months	still alive at 4 years and 6 months
Gender	female	male	female	female	male	male
Neurology						
Hypotonia (axial)	yes	yes	yes	yes	yes	yes
Hypertonia (limb)	not known	yes	yes	yes	yes	yes
Seizures	refractory focal seizures from 17 months	refractory focal seizures from 12 months, later development of epileptic spasms	epilepsy onset with febrile illness at 9 months	refractory infantile spasms, myoclonic and clonic seizures from 12 months	refractory epilepsy with tonic-clonic seizures, onset with febrile illness at 12 months	refractory epilepsy with myoclonic seizures and complex partial seizures, onset at 10 months
Developmental delay (DD)	mild-moderate DD to one year, then regression	mild-moderate DD to one year, then regression	normal development to 9 months, then rapid regression following seizure onset	mild DD in first year of life, then regression	normal development to 12 months, then rapid regression following seizure onset	mild DD to 12 months, then rapid regression with worsening of seizures
Brain MRI findings (age)	marked reduction of white matter volume, delayed myelination, thin corpus callosum (17 months)	marked reduction of white matter volume, delayed myelination, thin corpus callosum (17 months)	diffuse global white matter loss (9 months)	cerebral atrophy and delayed myelination (12 months)	cortical/gray matter atrophy, marked reduction of white matter volume, delayed myelination, corpus callosum hypoplasia (19 months)	severe cerebral and moderate cerebellar atrophy, periventricular leukomalacia, mild hypomyelination (16 months)
Cranial CT findings (age)	not performed	not performed	multiple scattered punctate calcifications in the periventricular, deep and subcortical white matter of both cerebral hemispheres (9 months)	not performed	sparse calcic and punctate-like hyperdensities in subcortical and periventricular areas (12 months)	small calcifications near gray-white matter junction in parietal regions (16 months)

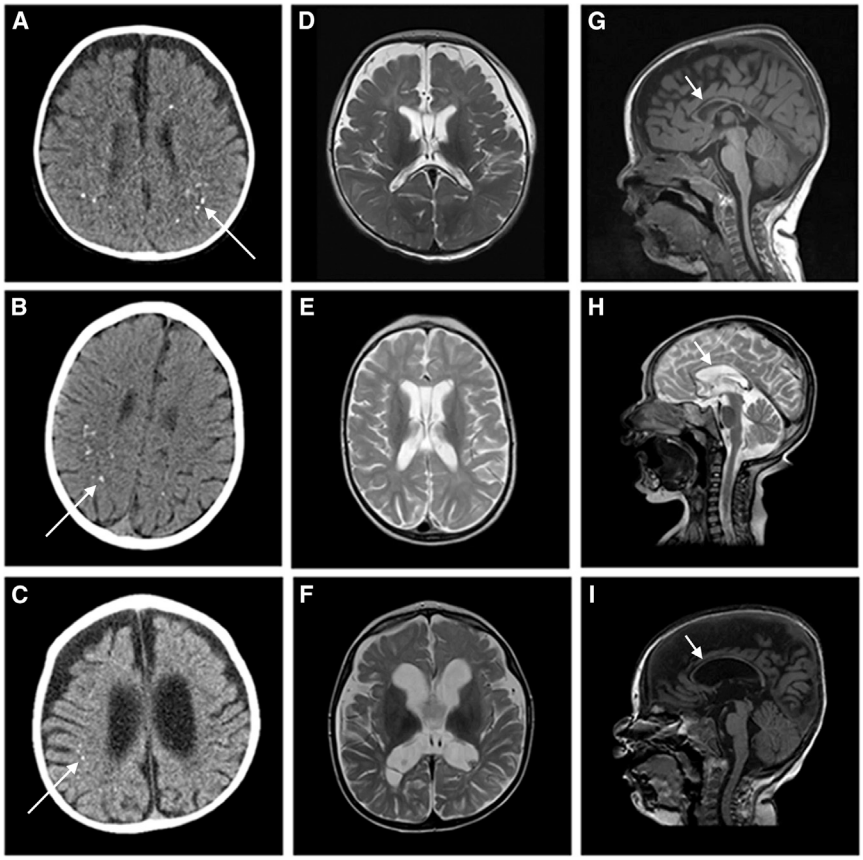

Figure 1. Brain MRI and CT for Affected Individuals with Bi-allelic *NRROS* Variants
(A, B, and C) Computed tomography (CT) brain imaging shows punctate calcification in subcortical and periventricular white matter (long arrow).
(D, E, and F) T2-weighted axial magnetic resonance imaging (MRI) brain imaging shows increased extra-axial spaces, reduced white matter volume, and delayed myelination.
(G, H, and I) Sagittal MRI brain imaging shows diffusely thin corpus callosum (short arrow).
Brain imaging of affected Individual II:4 in Family 1 (A, D, G) at age nine months; affected Individual II:3 in Family 3 (B, E, H) at ages 18 months (CT) and 19 months (MRI); and affected Individual II:2 in Family 4 (C, F, I) at age 16 months.

ventilatory support via tracheostomy. All individuals are non-dysmorphic. Brain magnetic resonance imaging (MRI) performed at nine to 19 months revealed marked cerebral atrophy and delayed myelination in all individuals, and it revealed corpus callosum hypoplasia in half. For all the individuals who had cranial computed tomography (CT) scans (three out of six), this imaging modality identified multiple sparse punctate calcifications of the cerebral white matter (Figure 1). Extensive investigations for other internal organ malformations were not pursued owing to a lack of suggestive clinical symptoms. Three individuals died between two and four years of age. The eldest surviving child is nine years old.

All procedures in this study were approved by and carried out in accordance with the ethical standards of the Human Ethics Committee of the Royal Children's Hospital, Melbourne, Victoria, Australia (HREC36291C) and the Ethics Committee of the Ospedale Pediatrico Bambino Gesù, Rome, Italy (1702_OPBG_2018). Affected individuals were recruited into Institutional Undiagnosed Diseases Programs for pediatric affected individuals with presumed "orphan" Mendelian disorders and subsequently put together through Matchmaker Exchange.[9] Saliva or blood samples from the affected individuals and their family members were collected for genomic DNA extraction after written informed consent was given. Whole-exome sequencing (WES) and data analyses were conducted for four individuals at Victorian Clinical Genetics Services (VCGS) in Australia (Families 1 and 2), for one individual at Ospedale Pediatrico Bambino Gesù in Italy (Family 3), and for one individual at Baylor College of Medicine in the United States (Family 4) (see Supplemental Material and Methods for details). Owing to the severity of refractory seizures for individuals II:2 and II:3 of Family 1 (Figure S1A), these individuals were initially enrolled in an epilepsy research study which did not identify a diagnosis in any known epilepsy genes via exome sequencing. Further research analysis of these two individuals identified the same homozygous deletion variant in *NRROS*, RefSeq accession number NM_198565.1, c.1981delC (p.Leu661Serfs*97). The same homozygous variant was then identified in another child of Iraqi background, II:2 of Family 2 (Figure S1B), who had research exome sequencing performed in order to investigate developmental regression and epilepsy. All three children were of Iraqi background and receiving care at the same tertiary pediatric institution. While the families do not report that their two families are related, they are presumed to be distantly related due to the overlap of their family histories, with ancestry originating from the same town in Iraq, and the identification of two overlapping regions of homozygosity on SNP microarray on chromosome 3q29 of 2.2 and 2.8 megabases, respectively. The more distal region of homozygosity on 3q29 contains the *NRROS* gene. Subsequently, another child, II:4, was born to the parents of Family 1, and in the context of seizures developing at nine months of age, II:4 was tested for the familial *NRROS* variant and was also found to be homozygous for the familial *NRROS* frameshift variant. The remaining two individuals, II:3 of Family 3 (Figure S1C) and II:2 of Family 4 (Figure S1D), were identified via Matchmaker Exchange.[9] Individual II:3 of Family 3 had been enrolled in the Undiagnosed Patients Program at the Ospedale

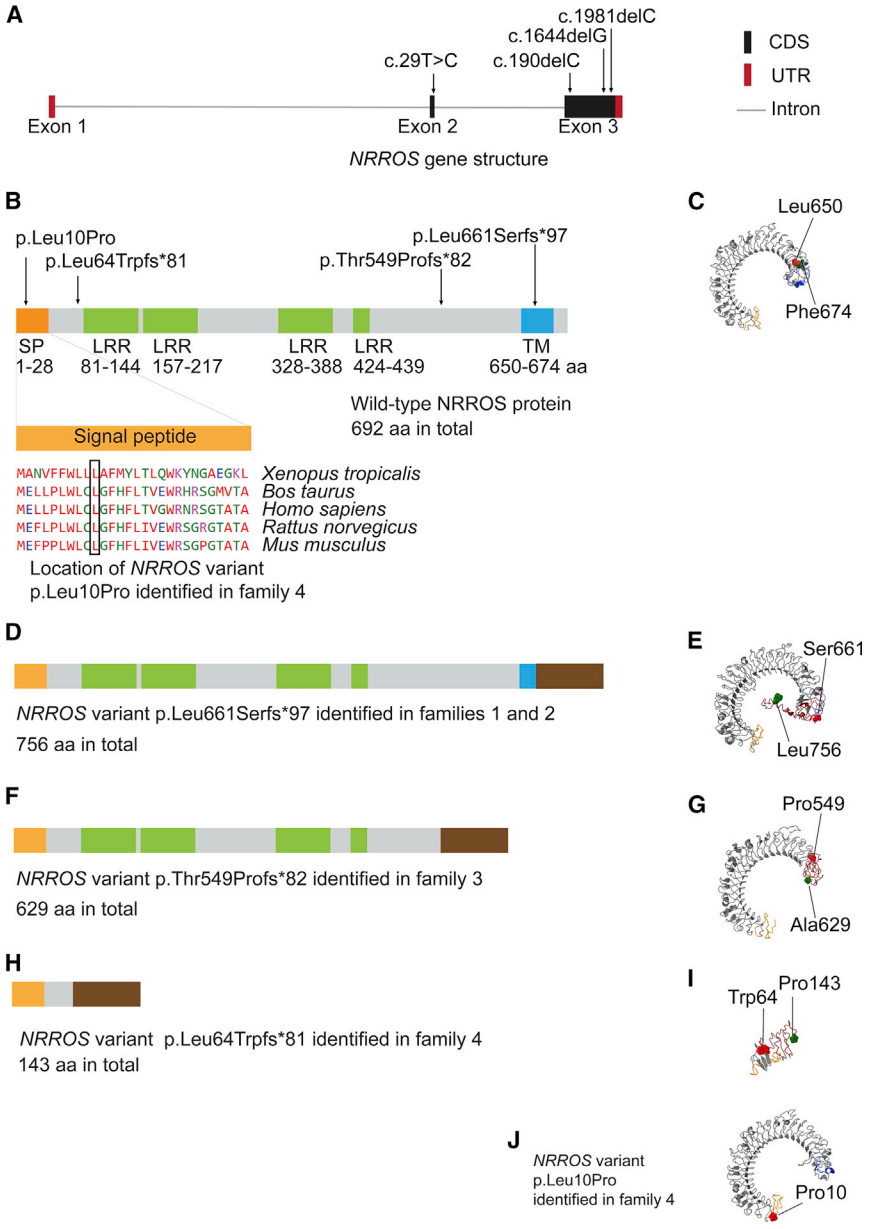

Figure 2. *NRROS* Gene, Protein Domain Structure, and Location of the Reported *NRROS* Variants

(A) Schematic diagram depicting the locations of variants identified in the *NRROS* gene. The gene structure information was obtained from the University of California Santa Cruz (UCSC) Genome Browser database.[11] The coding sequence (CDS; black), untranslated region (UTR; red), and intron (gray) are indicated.

(B) Schematic diagram depicting the locations of variants in wild-type NRROS protein. Protein structure was derived using Pfam. Signal peptide (SP; orange), four leucine-rich repeat (LRR) domains (green), and transmembrane segment (TM; blue) are indicated. Alignment of the NRROS signal peptide domain across multiple species indicates that the missense variant p.Leu10Pro affects a conserved amino acid residue. Multiple sequence alignment was performed using Clustal Omega[16] with reference to sequences for *Xenopus tropicalis* (RefSeq accession number NP_001231915.1), *Bos taurus* (RefSeq NP_001029563.1), *Homo sapiens* (RefSeq NP_940967.1), *Rattus norvegicus* (RefSeq NP_001020166.1), and *Mus musculus* (RefSeq NP_666181.2).

(C) Three-dimensional modeling of wild-type NRROS. For the transmembrane domain (TMD) in wild-type NRROS, the first amino acid of the domain (AA 650) is highlighted in red and the last amino acid (AA 674) is highlighted in green.

(D–I) Schematic diagrams depicting the predicted domain structure and three-dimensional modeling of *NRROS* variants p.Leu661Serfs*97 (D and E), p.Thr549Profs*82 (F and G), and p.Leu64Trpfs*81 (H and I).

(J) Three-dimensional modeling of *NRROS* variant p.Leu10Pro.

The NRROS TMD is indicated in blue, SP domain is labeled in orange, and frameshift changes are shown in brown (B to J). For the frameshift changes in mutant NRROS proteins, the first amino acids affected are colored in red and the last amino acids affected are colored in green (E, G, and I). The amino acid affected is colored in red in the missense *NRROS* variant p.Leu10Pro. All colored amino acids are shown in a space-fill model.

Pediatrico Bambino Gesù, Rome, Italy. A recessive trait was suspected owing to the clinical features documented in his sibling, who died at the age of four years due to a molecularly unclassified severe epileptic encephalopathy. The homozygous frameshift variant in *NRROS* (c.1644delG [p.Thr549Profs*82]) emerged as the only excellent candidate variant underlying the trait. Parents in all four families were heterozygous for the *NRROS* variants (Figure S1). Clinically unaffected siblings were either homozygous for the wild-type *NRROS* sequence or heterozygous carriers for an *NRROS* variant (Figure S1).

As listed in the University of California Santa Cruz (UCSC) Genome Browser and the Pfam database,[10,11] the *NRROS* gene has three exons, and the encoded protein includes a signal peptide (SP) domain (1–28 amino acids), four leucine-rich repeat (LRR) domains, and a transmembrane (TM) segment (Figures 2A and 2B). *In silico* modeling of wild-type and mutant NRROS proteins was performed using I-TASSER Suite.[12] Modeling prediction of wild-type NRROS shows that the transmembrane domain (TMD; blue) lies between leucine at position 650 (red) and phenylalanine at position 674 (green) (Figures 2C). The homozygous *NRROS* frameshift variant identified in Families 1 and 2 (p.Leu661Serfs*97) is predicted to result in substitution of leucine with serine at position 661 and creation of a new reading frame that results in termination after a divergent stretch of 97 residues. The resulting polypeptide lacks a relevant portion of the TMD (Figures 2D and 2E). The homozygous *NRROS* frameshift variant identified in Family 3 (p.Thr549Profs*82) is predicted to result

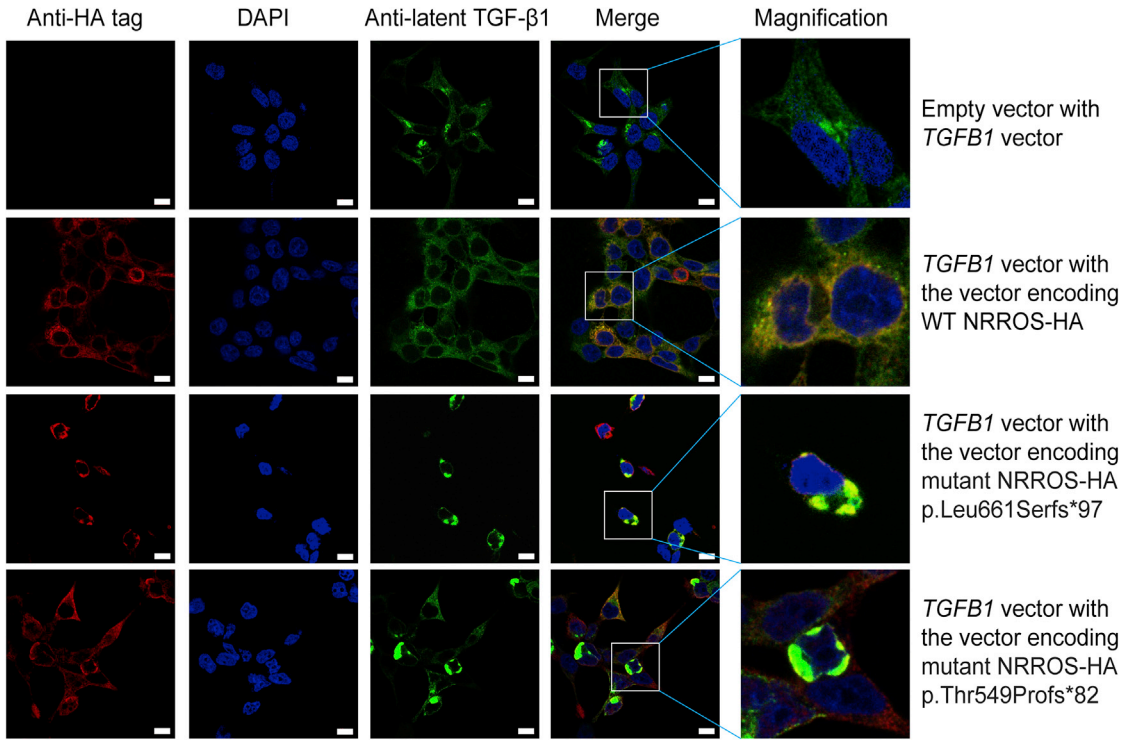

Figure 3. Co-localization of Latent TGF-β1 with Wild-Type or Mutant Hemagglutinin (HA)-tagged NRROS as Visualized by Confocal Microscopy

Confocal microscopy analysis of HEK293T cells co-transfected with a *TGFB1* expression vector and either an empty pcDNA3 vector or vectors encoding for wild-type or mutant NRROS-HA. Following transfection, cells were fixed for immunofluorescence staining with anti-HA (red) and anti-latent-TGF-β1 (green) antibodies. DAPI (blue) was used for nuclear staining. Scale bar: 10 μm. Data are representative of two independent experiments.

in a premature termination at position 629, with predicted loss of the entire TMD (Figures 2F and 2G). The affected individual from Family 4 (II:2) is compound heterozygous for two *NRROS* variants: one frameshift and one missense variant. The frameshift variant (p.Leu64Trpfs*81) is predicted to generate a severely truncated NRROS protein of only 143 amino acids (Figure 2H), lacking all four LRRs and the TMD (Figures 2H and 2I). The missense variant (p.Leu10Pro) is predicted to result in the substitution of Leu[10] (RefSeq NP_940967.1), a conserved residue that lies within the highly conserved SP domain (Figures 2B and 2J), and to affect proper protein sorting. The *in silico* prediction tool SignalP 5.0[13] was used to characterize signal peptide domains present in wild-type and missense mutant NRROS proteins. For the SP domain in wild-type NRROS, the probability score of being functional was predicted at 0.6559 (out of one), with a predicted cleavage site after glycine at position 18. This is consistent with UniProt protein database[14] information and with previously published literature[15] that reports a predicted signal peptide cleavage site in wild-type NRROS between amino acid positions 18 and 19. In contrast, the missense variant p.Leu10Pro was predicted to dramatically impact the SP domain's functionality (0.1256), and this suggests a loss-of-function related to defective intracellular transport and impaired secretion of the mutant protein (Figure S2).

NRROS is a membrane protein and has been found to localize on the endoplasmic reticulum (ER) and cell surface.[2,3] We examined the localization of mutant NRROS proteins by designing constructs bearing wild-type or representative *NRROS* variants (p.Leu661Serfs*97 and p.Thr549Profs*82) that carry a human influenza hemagglutinin (HA) at the C terminus. Western blot analysis indicated that all of the HA-tagged NRROS proteins had the expected molecular weights (Figure S3). To examine proper localization of NRROS at the ER membrane, we transfected HEK293T cells with each of the *NRROS* expression vectors and we performed immunostaining with anti-HA and anti-calnexin antibodies. Both wild-type and mutant NRROS were found to co-localize with the ER marker calnexin in a similar manner (Figure S4).

Wild-type NRROS has been observed to play an important role in TGF-β signaling in myeloid cells via interaction with latent TGF-β1.[2] To investigate this interaction, we transfected HEK293T cells with a *TGFB1* expression vector encoding for latent TGF-β1, together with *NRROS* expression vectors encoding for wild-type and mutant HA-tagged NRROS proteins. Using confocal microscopy, we observed the co-localization of latent TGF-β1 with wild-type and mutant HA-tagged NRROS within cells following intracellular staining, indicating that latent TGF-β1 interacts with both wild-type NRROS and mutant NRROS proteins (Figure 3). Notably, we observed the formation of latent

TGF-β1-positive aggregates upon the expression of *TGFB1* alone or with mutant *NRROS*, suggesting that proper folding and/or transportation of latent TGF-β1 might require wild-type NRROS (see magnified images in Figure 3).

Two proteins, leucine-rich repeat-containing protein 32 (LRRC32) and NRROS, bind and anchor latent TGF-β1 to the cell surface for TGF-β1 activation.[2,17] They both contain a transmembrane domain and LRRs with approximately 35% sequence homology.[17] Twenty-eight of 56 residues in LRRC32 involved in disulfide-mediated tethering of latent TGF-β1 are found to be conserved in the NRROS protein.[17] Recently, a homozygous stop-gain variant in *LRRC32* (MIM: 137207) has been reported in association with a multisystem disorder with developmental delay.[18] The three affected individuals from two families were reported to have cleft palate, proliferative retinopathy, and developmental delay. The stop-gain variant was predicted to result in a truncated LRRC32 protein that lacks the transmembrane domain, the same consequence as was predicted for our frameshift *NRROS* variants. The phenotype reported by Harel et al.[18] differs significantly from that of our cohort and might be explained by the differing tissue levels for LRRC32 and NRROS. While NRROS protein levels are high in myeloid cells, including microglia, *LRRC32* is expressed at a very low level.[2] To analyze the influence of mutant NRROS proteins in anchoring latent TGF-β1 to the cell surface, we performed flow cytometry. Upon co-expression of *TGFB1* with wild-type or mutant HA-tagged *NRROS*, HEK293T cells were subjected to both cell surface and intracellular staining for flow cytometry analysis. Co-transfection of the *TGFB1* expression vector together with wild-type or mutant *NRROS* vectors led to a similar percentage of HEK293T cells with intracellular latent TGF-β1, as well as those with double positive intracellular staining by anti-human LAP (TGF-β1) and anti-HA antibodies (Figures 4A and 4B and Figure S5A). Co-transfection of HEK293T cells with the *TGFB1* expression vector and the empty pcDNA3 vector resulted in approximately 6% of living cells with surface staining of latent TGF-β1. In contrast, approximately 21% of living cells demonstrated cell-surface-latent TGF-β1 when overexpressing *TGFB1* along with wild-type *NRROS*, implying that wild-type NRROS can deliver more latent TGF-β1 to the cell surface in addition to endogenous NRROS in HEK293T cells (Figure 4C and Figure S5B). Remarkably, an extremely small number of cells showed cell surface staining of latent TGF-β1 upon co-overexpression of *TGFB1* with each of the two disease-associated *NRROS* variants, suggesting that mutant NRROS may sequester latent TGF-β1 intracellularly or affect proper folding of latent TGF-β1, thus impairing the presentation of latent TGF-β1 on the cell surface (Figure 4C and Figure S5B).

In *Nrros* knockout mouse models, heterozygous mice were healthy, whereas homozygous *Nrros* knockout mice showed impaired motor function and neurodegeneration with abnormal microglial development and microgliosis.[2,5] In this study, heterozygous carriers for *NRROS* variants were unaffected, as well. Thus, we hypothesized that wild-type NRROS can rescue the mutant NRROS-mediated depletion of latent TGF-β1 on the cell surface. Wild-type and mutant NRROS were distinguished by fusing a MYC tag to the wild-type *NRROS* construct (Figure S3). Intracellular staining showed that similar proportions of cells were positive for both latent TGF-β1 and HA-tag staining upon co-expression of *TGFB1* and HA-tagged mutant *NRROS*, with or without wild-type MYC-tagged *NRROS* (Figure 4D and Figure S6A). Moreover, a comparable number of cells were positive for the intracellular MYC-tag or latent TGF-β1 staining upon co-expression of wild-type MYC-tagged *NRROS* and *TGFB1*, with or without mutant HA-tagged *NRROS* (Figure 4E and Figures S6A, S6B and S7A). Overexpression of wild-type *NRROS* with *TGFB1* and mutant *NRROS* succeeded in presenting latent TGF-β1 to the cell surface, in comparison to the empty pcDNA3 vector (Figure 4F and Figure S6C). The rescued presentation of cell-surface-latent TGF-β1 occurred at a level largely achieved by cells expressing only wild-type *NRROS* and *TGFB1* (Figure 4F and Figure S6C).

In the present study, the two *NRROS* frameshift variants (p.Leu661Serfs*97 and p.Thr549Profs*82) retain all of the conserved residues required for the interaction of NRROS with latent TGF-β1. Due to partial or complete loss of the TMD, these mutant NRROS proteins fail to present latent TGF-β1 to the cell surface. The third *NRROS* frameshift variant, p.Leu64Trpfs*81, is not only predicted to fail to anchor latent TGF-β1 to the cell surface due to the loss of the TMD, but also predicted to be unable to bind to latent TGF-β1 due to the complete loss of the conserved residues that interact with latent TGF-β1. Genetic variants that affect signal peptide domains have been found to disrupt cellular localization and protein function, and these variants are often missense in nature.[19] The *NRROS* missense variant p.Leu10Pro lies within the signal peptide domain of NRROS and is predicted to affect protein transport (Figure S2). The amino acid substitutions of leucine to proline in the SPs of other proteins often affect protein localization and secretion.[20–22] In this study, the individual harboring this missense variant was found to be a compound heterozygote with the *NRROS* frameshift variant p.Leu64Trpfs*81. He presents with similar phenotypic features to those of the remaining individuals studied, all of whom had homozygous frameshift variants that have demonstrated reduced capacity to deliver latent TGF-β1 to the cell surface. Segregation testing of this affected individual revealed bi-allelic inheritance of the compound heterozygous variants from clinically unaffected carrier parents. Thus, the missense variant, when in compound heterozygous state with another *NRROS* frameshift variant, is predicted to result in impaired NRROS-mediated transport of latent TGF-β1.

In summary, the reported frameshift and missense variants are predicted to impact proper targeting of NRROS

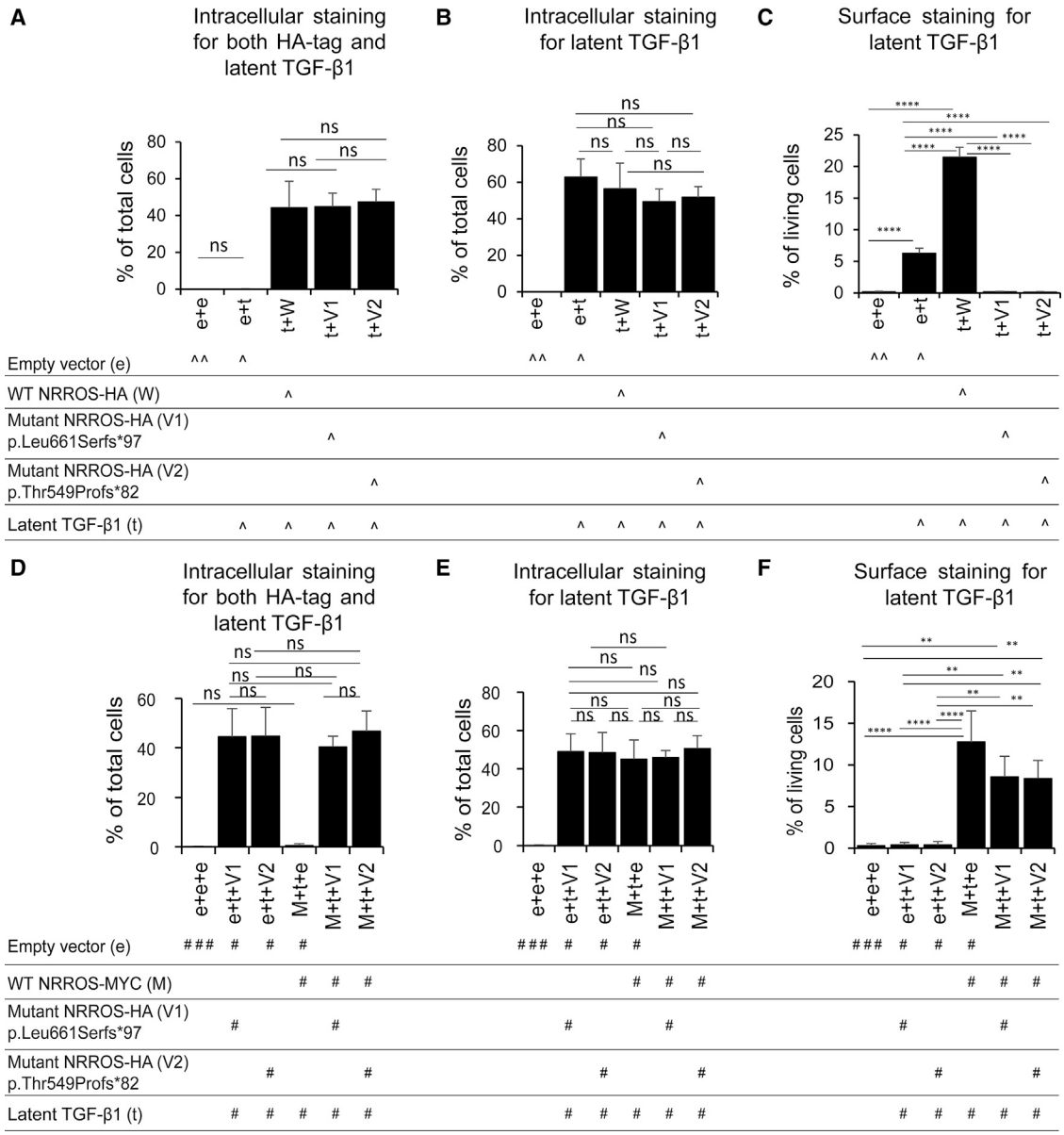

Figure 4. Flow Cytometry Analysis of Intracellular and Cell Surface Staining of Latent TGF-β1 Influenced by Mutant NRROS Alone or Together with Wild-Type NRROS in HEK293T Cells after Transfection

(A) The percentage of total cells with intracellular staining for both hemagglutinin (HA)-tagged and latent TGF-β1 after transfection with different vectors for indicated proteins.

(B) The percentage of total cells with intracellular staining for latent TGF-β1.

(C) The percentage of living cells with latent TGF-β1 staining on the cell surface.

(D) The percentage of total cells with intracellular staining for both HA-tagged and latent TGF-β1.

(E) The percentage of total cells with intracellular staining for latent TGF-β1.

(F) The percentage of living cells with latent TGF-β1 staining on the cell surface.

Data are presented as the mean ± standard deviation of three independent experiments (n = 3), and a one-way ANOVA analysis with a Tukey's post hoc honestly significant difference (HSD) test was performed to calculate p values. **$p < 0.01$, ****$p < 0.0001$. ns—not significant, e—the empty vector, t—the vector encoding latent TGF-β1, W—the vector encoding wild-type NRROS-HA, V1—the vector encoding HA-tagged mutant NRROS p.Leu661Serfs*97, V2—the vector encoding HA-tagged mutant NRROS p.Thr549Profs*82, M—the vector encoding wild-type NRROS-MYC, +—along with, ^—250 ng plasmid DNA, #—200 ng plasmid DNA.

and impair the ability to anchor latent TGF-β1 on the cell surface, which is required for activation of TGF-β1 signaling. We have shown that wild-type NRROS can transport latent TGF-β1 to the cell surface (Figure 5A), while disease-causing NRROS mutants have impaired ability to anchor latent TGF-β1 to the cell surface (Figure 5B). Significantly, wild-type NRROS can rescue mutant NRROS-mediated depletion of latent TGF-β1 at the cell surface.

We postulate that aberrant NRROS protein has an impaired ability to anchor latent TGF-β1 on the cell surface, resulting in perturbed bioavailability of active TGF-β

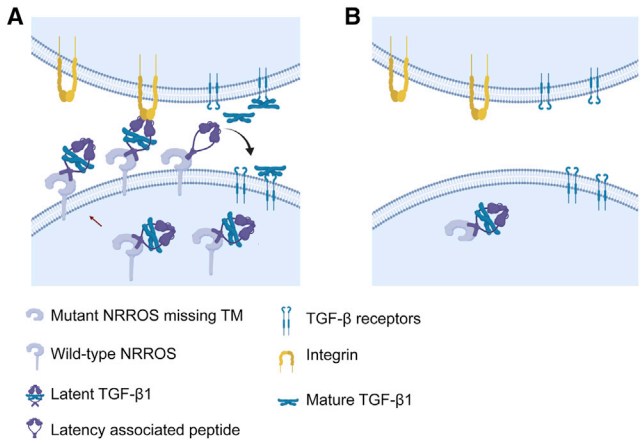

Figure 5. A Model of Latent TGF-β1 Presentation on the Cell Surface, Mediated by Wild-Type NRROS or Mutant NRROS with an Absent Transmembrane Domain

(A) Wild-type NRROS directs intracellular synthesis and processing of latent TGF-β1 to the cell surface, where it is then subject to integrin-dependent release of active TGF-β1.

(B) *NRROS* variants with an impaired or missing transmembrane domain fail to anchor NRROS-latent TGF-β1 complexes on the cell surface, resulting in failure to release active TGF-β1, which in turn leads to defective TGF-β1 signaling.

leading to dysregulated TGF-β signaling. The neurologic phenotype in the reported individuals is similar to that seen in individuals with bi-allelic *TGFB1* loss-of-function variants.[23] The overlapping features include cortical atrophy, delayed myelination, corpus callosum hypoplasia, developmental regression, and refractory epilepsy. The experimental findings by Kotlarz and colleagues suggest that perturbed bioavailability of TGF-β1 may be the underlying pathomechanism for affected individuals with bi-allelic variants in *TGFB1*,[23] which is a similar pathology hypothesized here for the individuals with bi-allelic variants in *NRROS*. Several binding partners of latent TGF-β1 mediate the activation of TGF-β signaling, and these include latent transforming growth factor β binding proteins (LTBPs), LRRC32, and NRROS.[2] The phenotypes associated with dysregulated TGF-β signaling will likely differ depending on the defective binding partner involved owing to differential tissue levels of these proteins. Protein levels of LTBPs and LRRC32 are very low in microglia, as opposed to NRROS.[2] Thus, the phenotype associated with aberrant NRROS function might be expected to be more pronounced in the CNS than are disorders associated with deficiencies of other latent TGF-β1 binding partners.

Following CNS infection or injury, microglial cells are activated and recruited to come to pathogens or injured cells to mediate phagocytosis and release of substances such as pro-inflammatory cytokines.[24] Notably, TGF-β1 plays important roles in the survival of neural cells and inhibition of induced microglial activation and associated inflammatory cytokine production.[25,26] Although ordinarily there is a small amount of TGF-β1 in healthy adult neural cells, it can be rapidly upregulated to protect neuronal cells against brain injury in response to neuronal insults such as inflammatory molecules and oxidative products, especially in microglia.[8,27,28] We propose that a lack of functional NRROS protein may result in uncontrolled microglial activation owing to the loss of TGF-β1 inhibitory activity, because mutant NRROS has an impaired ability to anchor latent TGF-β1 to the cell surface and thus has impaired release of active TGF-β1. In theory, unchecked activation of microglia could lead to microgliosis, chronic neuroinflammatory responses, elevated ROS production, and neuronal cell death. In support of this theory, cerebrospinal fluid (CSF) testing for Individual II:4 from Family 1 detected elevated CSF neopterin, which is suggestive of CNS inflammation. Similarly, one of the affected individuals reported by Kotlarz and colleagues[23] had CSF testing that identified oligoclonal IgG bands and increased levels of the interleukin IL-1β, which is also suggestive of a neuroinflammatory process. In addition, all affected individuals in this report exhibited a reduction of white matter volume over time, and this reduction may be secondary to neuronal cell death. Taken together, these results suggest that neuroinflammation and neuronal cell death are features of the downstream effect of insufficient TGF-β1 activation caused by *NRROS* variants. Our proposed pathomechanism in NRROS deficiency differs from that of the chronic neuroinflammation implicated in other neurodegenerative conditions such as Alzheimer's disease, Parkinson's disease, and frontotemporal dementia. In these adult-onset neurodegenerative conditions, it is thought that the continual activation of microglia is mediated by insidious exposure to proinflammatory stimuli, such as amyloid-beta plaques in Alzheimer's disease.[29]

Intracranial calcification (ICC) was identified in three of the six individuals in this study. ICC refers to calcification within the cranial cavity, which is generally accepted to mean the brain parenchyma or its vasculature.[30] There are several hypotheses to explain calcium deposition in the brain; these hypotheses include abnormal calcium metabolism,[31] microangiopathy,[32] and inflammation.[33] ICC has not yet been examined in *Nrros* knockout mice. ICC is associated with a highly heterogeneous clinical presentation, the major categories of which include physiologic, dystrophic, and congenital disorders and infectious, vascular, neoplastic, metabolic/endocrine, inflammatory, and toxic diseases.[34] Normal age-related physiological calcification is thought to occur largely in the pineal gland and choroid plexus, and even so, it rarely occurs within the first two decades of life. Thus, ICC manifesting in childhood can be considered to be pathological. Evaluation of affected individual age along with localization of calcification is paramount when considering the differential diagnosis of pathologic ICC. ICC can be associated with dystrophic processes such as ischemic injury secondary to stroke. Several congenital infections manifest with ICC; these include cytomegalovirus, herpes simplex virus, toxoplasmosis, rubella, Zika virus, and HIV. Vascular calcifications can be seen in the context of atherosclerotic lesions and vascular malformations such as cavernous angiomas and arteriovenous malformations. The presence

and distribution of calcification in brain neoplasms is important for delineating intracranial tumors. Metabolic and endocrine disorders affecting calcium homeostasis may lead to intracranial calcium deposition, as has been seen with hypoparathyroidism, hyperparathyroidism, and hypothyroidism. Inflammatory conditions such as systemic lupus erythematosus and sarcoidosis demonstrate ICC, and neurotoxic agents such as lead and carbon monoxide have also been responsible for the development of ICC. Finally, there are several monogenic disorders for which ICC is a feature; these include tuberous sclerosis, neurofibromatosis, and Sturge-Weber syndrome. Examples of genetic neurodegenerative diseases with ICC include Cockayne syndrome (MIM: 216400; MIM: 133540), Krabbe disease (MIM: 245200), X-linked adrenoleukodystrophy (MIM: 300100), Alexander disease (MIM: 203450), Fabry disease (MIM: 301500), and mitochondrial disease. One of the best described conditions with ICC is Aicardi-Goutieres syndrome (AGS), a type 1 interferonopathy caused by variants in a number of genes:[35] *TREX1* (MIM: 606609), *RNASEH2B* (MIM: 610326), *RNASEH2C* (MIM: 610330), *RNASEH2A* (MIM: 606034), *SAMHD1* (MIM: 606754), *ADAR* (MIM: 146920), and *IFIH1* (MIM: 606951). AGS presents as an early-onset encephalopathy that most commonly results in severe intellectual and physical disability.[36] The ICC in AGS is postulated to be the result of neuroinflammation[33] which, as has been suggested here, is also the possible cause for the affected individuals in this cohort. As such, pathogenic variants in *NRROS* should be considered in the list of differential diagnoses for ICC.

There is some evidence to suggest that microglial dysregulation leads to neurological disease and cerebral calcification. Mice with depletion of Usp18, a negative regulator of microglia activation, demonstrate ICC, which is also a feature in human USP18 deficiency.[37,38] ICC has also been identified in affected individuals with mutations in other genes that play important roles in microglial development and function, such as *IRF8* (MIM: 601565), *CSF1R* (MIM: 164770), and *PDGFB* (MIM: 190040).[39–41] Recently, a *Pdgfb* knockout mouse model of primary familial brain calcification has been used to investigate the hypothesized association of microglial dysregulation with ICC formation.[42] Microglia depletion in *Pdgfb* knockout mice using the CSF1R inhibitor PLX5622 resulted in aggravated intracranial vessel calcification, which suggests a protective role for microglia in the development of ICC.

A possible treatment strategy is bone marrow (BM) transplantation. Hematopoietic cells in BM can migrate into the CNS and differentiate into microglia. BM transplantation has been used to rescue microglia-related CNS pathologies by restoring functional microglia.[43] Notably, BM transplantation has been effective in slowing down or stopping clinical symptom progression in 12-week-old *Nrros* knockout mice. This raises the potential for future therapeutic options for this neurological disorder.[2,7] Identification of other treatment strategies may include the use of high throughput chemical screening to help identify ways to rescue defective TGF-β1 delivery via other TGF-β1 binding partners or chaperone molecules.

It is necessary to be aware of the limitations in this study. We fused small peptide tags including HA or MYC to the C terminus of wild-type and aberrant NRROS proteins, and we transfected cells with plasmids encoding these fusion proteins for immunostaining and flow cytometry analysis. Overexpression studies may not represent physiologic phenomena because these studies generate supraphysiological protein levels, which may complicate interpretation as a consequence of dysregulation of biological pathways, interference with the assembly of protein complexes, or cytotoxicity.[44,45] While it is generally assumed that small protein tags used in biochemical experiments have minimal impact on their tagged protein,[46] it has been reported that adding small tags may affect protein stability,[46,47] function, or interaction.[44,48] Thus, cautious analysis is needed and further investigation is warranted.

In conclusion, our studies suggest that germline bi-allelic loss-of-function variants in the *NRROS* gene cause a severe monogenic infantile onset neurodegenerative disorder characterized by neurodegeneration and epilepsy, with features suggestive of neuroinflammation. We show that aberrant NRROS function results in impaired delivery of active TGF-β1, and we hypothesize that impaired TGF-β1 activation is a major contributor to the phenotypes in these affected individuals.

Supplemental Data

Supplemental Data can be found online at https://doi.org/10.1016/j.ajhg.2020.02.014.

Acknowledgments

We are grateful to the affected individuals and their family members for participating in this study. We thank Shahnaz Khan for providing the Calnexin antibody. We also thank Joseph Tam for his support with clinical information provided. The research conducted at the Murdoch Children's Research Institute was supported by the Victorian Government's Operational Infrastructure Support Program. We are grateful to the Harbig Foundation for generous financial support. N.T. acknowledges the Australian National Health and Medical Research Council (NHMRC) Centre for Research Excellence in Neurocognitive Disorders for their support. K.B.H. is supported by funding from the Australian NHMRC. M.T. acknowledges the Italian Ministry of Health (Ricerca Corrente 2019) and Fondazione Bambino Gesù (Vite Coraggiose).

Declaration of Interests

The authors declare no competing interests.

Received: December 25, 2019
Accepted: February 26, 2020
Published: March 19, 2020

Web Resources

Clustal Omega, https://www.ebi.ac.uk/Tools/msa/clustalo/
ExAC Browser, http://exac.broadinstitute.org/
Genome Aggregation Database (gnomAD), https://gnomad.broadinstitute.org/
I-TASSER, https://zhanglab.ccmb.med.umich.edu/I-TASSER/
Matchmaker Exchange, https://www.matchmakerexchange.org/
Mutation Taster, http://www.mutationtaster.org/
NCBI Primer-BLAST, https://www.ncbi.nlm.nih.gov/tools/primer-blast/
OMIM, https://omim.org/
Pfam, https://pfam.xfam.org/
SIFT, https://sift.bii.a-star.edu.sg/
SignalP-5.0, http://www.cbs.dtu.dk/services/SignalP/
UCSC Genome Browser, https://genome.ucsc.edu/

References

1. Ng, A., and Xavier, R.J. (2011). Leucine-rich repeat (LRR) proteins: integrators of pattern recognition and signaling in immunity. Autophagy *7*, 1082–1084.
2. Qin, Y., Garrison, B.S., Ma, W., Wang, R., Jiang, A., Li, J., Mistry, M., Bronson, R.T., Santoro, D., Franco, C., et al. (2018). A Milieu Molecule for TGF-beta Required for Microglia Function in the Nervous System. Cell *174*, 156–171.
3. Noubade, R., Wong, K., Ota, N., Rutz, S., Eidenschenk, C., Valdez, P.A., Ding, J., Peng, I., Sebrell, A., Caplazi, P., et al. (2014). NRROS negatively regulates reactive oxygen species during host defence and autoimmunity. Nature *509*, 235–239.
4. Kim, J.H., Kim, K., Kim, I., Seong, S., and Kim, N. (2015). NRROS Negatively Regulates Osteoclast Differentiation by Inhibiting RANKL-Mediated NF-N:B and Reactive Oxygen Species Pathways. Mol. Cells *38*, 904–910.
5. Wong, K., Noubade, R., Manzanillo, P., Ota, N., Foreman, O., Hackney, J.A., Friedman, B.A., Pappu, R., Scearce-Levie, K., and Ouyang, W. (2017). Mice deficient in NRROS show abnormal microglial development and neurological disorders. Nat. Immunol. *18*, 633–641.
6. Ma, W., Qin, Y., Chapuy, B., and Lu, C. (2019). LRRC33 is a novel binding and potential regulating protein of TGF-β1 function in human acute myeloid leukemia cells. PLoS ONE *14*, e0213482.
7. Brionne, T.C., Tesseur, I., Masliah, E., and Wyss-Coray, T. (2003). Loss of TGF-beta 1 leads to increased neuronal cell death and microgliosis in mouse brain. Neuron *40*, 1133–1145.
8. Butovsky, O., Jedrychowski, M.P., Moore, C.S., Cialic, R., Lanser, A.J., Gabriely, G., Koeglsperger, T., Dake, B., Wu, P.M., Doykan, C.E., et al. (2014). Identification of a unique TGF-β-dependent molecular and functional signature in microglia. Nat. Neurosci. *17*, 131–143.
9. Philippakis, A.A., Azzariti, D.R., Beltran, S., Brookes, A.J., Brownstein, C.A., Brudno, M., Brunner, H.G., Buske, O.J., Carey, K., Doll, C., et al. (2015). The Matchmaker Exchange: a platform for rare disease gene discovery. Hum. Mutat. *36*, 915–921.
10. Finn, R.D., Bateman, A., Clements, J., Coggill, P., Eberhardt, R.Y., Eddy, S.R., Heger, A., Hetherington, K., Holm, L., Mistry, J., et al. (2014). Pfam: the protein families database. Nucleic Acids Res. *42*, D222–D230.
11. Karolchik, D., Hinrichs, A.S., and Kent, W.J. (2007). The UCSC Genome Browser. Current Protocols in Bioinformatics *17*, 1.4.1–1.4.24. https://doi.org/10.1002/0471250953.bi0104s17.
12. Yang, J., Yan, R., Roy, A., Xu, D., Poisson, J., and Zhang, Y. (2015). The I-TASSER Suite: protein structure and function prediction. Nat. Methods *12*, 7–8.
13. Almagro Armenteros, J.J., Tsirigos, K.D., Sønderby, C.K., Petersen, T.N., Winther, O., Brunak, S., von Heijne, G., and Nielsen, H. (2019). SignalP 5.0 improves signal peptide predictions using deep neural networks. Nat. Biotechnol. *37*, 420–423.
14. UniProt Consortium (2008). The universal protein resource (UniProt). Nucleic Acids Res. *36*, D190–D195.
15. Liu, J., Zhang, Z., Chai, L., Che, Y., Min, S., and Yang, R. (2013). Identification and characterization of a unique leucine-rich repeat protein (LRRC33) that inhibits Toll-like receptor-mediated NF-κB activation. Biochem. Biophys. Res. Commun. *434*, 28–34.
16. Sievers, F., Wilm, A., Dineen, D., Gibson, T.J., Karplus, K., Li, W., Lopez, R., McWilliam, H., Remmert, M., Söding, J., et al. (2011). Fast, scalable generation of high-quality protein multiple sequence alignments using Clustal Omega. Mol. Syst. Biol. *7*, 539.
17. Liénart, S., Merceron, R., Vanderaa, C., Lambert, F., Colau, D., Stockis, J., van der Woning, B., De Haard, H., Saunders, M., Coulie, P.G., et al. (2018). Structural basis of latent TGF-β1 presentation and activation by GARP on human regulatory T cells. Science *362*, 952–956.
18. Harel, T., Levy-Lahad, E., Daana, M., Mechoulam, H., Horowitz-Cederboim, S., Gur, M., Meiner, V., and Elpeleg, O. (2019). Homozygous stop-gain variant in LRRC32, encoding a TGFβ receptor, associated with cleft palate, proliferative retinopathy, and developmental delay. Eur. J. Hum. Genet. *27*, 1315–1319.
19. Jarjanazi, H., Savas, S., Pabalan, N., Dennis, J.W., and Ozcelik, H. (2008). Biological implications of SNPs in signal peptide domains of human proteins. Proteins *70*, 394–403.
20. Symoens, S., Malfait, F., Renard, M., André, J., Hausser, I., Loeys, B., Coucke, P., and De Paepe, A. (2009). COL5A1 signal peptide mutations interfere with protein secretion and cause classic Ehlers-Danlos syndrome. Hum. Mutat. *30*, E395–E403.
21. Laurila, K., and Vihinen, M. (2009). Prediction of disease-related mutations affecting protein localization. BMC Genomics *10*, 122.
22. Chyra Kufova, Z., Sevcikova, T., Januska, J., Vojta, P., Boday, A., Vanickova, P., Filipova, J., Growkova, K., Jelinek, T., Hajduch, M., and Hajek, R. (2018). Newly designed 11-gene panel reveals first case of hereditary amyloidosis captured by massive parallel sequencing. J. Clin. Pathol. *71*, 687–694.
23. Kotlarz, D., Marquardt, B., Barøy, T., Lee, W.S., Konnikova, L., Hollizeck, S., Magg, T., Lehle, A.S., Walz, C., Borggraefe, I., et al. (2018). Human TGF-β1 deficiency causes severe inflammatory bowel disease and encephalopathy. Nat. Genet. *50*, 344–348.
24. Domercq, M., Vázquez-Villoldo, N., and Matute, C. (2013). Neurotransmitter signaling in the pathophysiology of microglia. Front. Cell. Neurosci. *7*, 49.
25. Chen, X., Liu, Z., Cao, B.B., Qiu, Y.H., and Peng, Y.P. (2017). TGF-β1 Neuroprotection via Inhibition of Microglial Activation in a Rat Model of Parkinson's Disease. J. Neuroimmune Pharmacol. *12*, 433–446.
26. Zhou, X., Zöller, T., Krieglstein, K., and Spittau, B. (2015). TGFβ1 inhibits IFNγ-mediated microglia activation and protects mDA neurons from IFNγ-driven neurotoxicity. J. Neurochem. *134*, 125–134.

27. Flanders, K.C., Ren, R.F., and Lippa, C.F. (1998). Transforming growth factor-betas in neurodegenerative disease. Prog. Neurobiol. *54*, 71–85.
28. Finch, C.E., Laping, N.J., Morgan, T.E., Nichols, N.R., and Pasinetti, G.M. (1993). TGF-beta 1 is an organizer of responses to neurodegeneration. J. Cell. Biochem. *53*, 314–322.
29. Bachiller, S., Jiménez-Ferrer, I., Paulus, A., Yang, Y., Swanberg, M., Deierborg, T., and Boza-Serrano, A. (2018). Microglia in Neurological Diseases: A Road Map to Brain-Disease Dependent-Inflammatory Response. Front. Cell. Neurosci. *12*, 488.
30. Livingston, J.H., Stivaros, S., Warren, D., and Crow, Y.J. (2014). Intracranial calcification in childhood: a review of aetiologies and recognizable phenotypes. Dev. Med. Child Neurol. *56*, 612–626.
31. Goswami, R., Sharma, R., Sreenivas, V., Gupta, N., Ganapathy, A., and Das, S. (2012). Prevalence and progression of basal ganglia calcification and its pathogenic mechanism in patients with idiopathic hypoparathyroidism. Clin. Endocrinol. (Oxf.) *77*, 200–206.
32. Shanley, D.J. (1995). Mineralizing microangiopathy: CT and MRI. Neuroradiology *37*, 331–333.
33. Crow, Y.J., and Manel, N. (2015). Aicardi-Goutières syndrome and the type I interferonopathies. Nat. Rev. Immunol. *15*, 429–440.
34. Saade, C., Najem, E., Asmar, K., Salman, R., El Achkar, B., and Naffaa, L. (2019). Intracranial calcifications on CT: an updated review. J. Radiol. Case Rep. *13*, 1–18.
35. Crow, Y.J., Chase, D.S., Lowenstein Schmidt, J., Szynkiewicz, M., Forte, G.M., Gornall, H.L., Oojageer, A., Anderson, B., Pizzino, A., Helman, G., et al. (2015). Characterization of human disease phenotypes associated with mutations in TREX1, RNASEH2A, RNASEH2B, RNASEH2C, SAMHD1, ADAR, and IFIH1. Am. J. Med. Genet. A. *167A*, 296–312.
36. Crow, Y.J. (1993). Aicardi-Goutieres Syndrome. In GeneReviews, M.P. Adam, H.H. Ardinger, R.A. Pagon, S.E. Wallace, L.J.H. Bean, K. Stephens, and A. Amemiya, eds. (Seattle (WA): University of Washington, Seattle), pp. 1993–2020.
37. Goldmann, T., Zeller, N., Raasch, J., Kierdorf, K., Frenzel, K., Ketscher, L., Basters, A., Staszewski, O., Brendecke, S.M., Spiess, A., et al. (2015). USP18 lack in microglia causes destructive interferonopathy of the mouse brain. EMBO J. *34*, 1612–1629.
38. Meuwissen, M.E., Schot, R., Buta, S., Oudesluijs, G., Tinschert, S., Speer, S.D., Li, Z., van Unen, L., Heijsman, D., Goldmann, T., et al. (2016). Human USP18 deficiency underlies type 1 interferonopathy leading to severe pseudo-TORCH syndrome. J. Exp. Med. *213*, 1163–1174.
39. Bigley, V., Maisuria, S., Cytlak, U., Jardine, L., Care, M.A., Green, K., Gunawan, M., Milne, P., Dickinson, R., Wiscombe, S., et al. (2018). Biallelic interferon regulatory factor 8 mutation: A complex immunodeficiency syndrome with dendritic cell deficiency, monocytopenia, and immune dysregulation. J. Allergy Clin. Immunol. *141*, 2234–2248.
40. Daida, K., Nishioka, K., Li, Y., Nakajima, S., Tanaka, R., and Hattori, N. (2017). CSF1R Mutation p.G589R and the Distribution Pattern of Brain Calcification. Intern. Med. *56*, 2507–2512.
41. Keller, A., Westenberger, A., Sobrido, M.J., García-Murias, M., Domingo, A., Sears, R.L., Lemos, R.R., Ordoñez-Ugalde, A., Nicolas, G., da Cunha, J.E., et al. (2013). Mutations in the gene encoding PDGF-B cause brain calcifications in humans and mice. Nat. Genet. *45*, 1077–1082.
42. Zarb, Y., Nassiri, S., Utz, S.G., Schaffenrath, J., Rushing, E.J., Nilsson, K.P.R., Delorenzi, M., Colonna, M., Greter, M., and Keller, A. (2019). Microglia 1 control small vessel calcification via TREM2. bioRxiv. https://doi.org/10.1101/829341.
43. Wirenfeldt, M., Babcock, A.A., and Vinters, H.V. (2011). Microglia - insights into immune system structure, function, and reactivity in the central nervous system. Histol. Histopathol. *26*, 519–530.
44. Berggård, T., Linse, S., and James, P. (2007). Methods for the detection and analysis of protein-protein interactions. Proteomics *7*, 2833–2842.
45. Prelich, G. (2012). Gene overexpression: uses, mechanisms, and interpretation. Genetics *190*, 841–854.
46. Saiz-Baggetto, S., Méndez, E., Quilis, I., Igual, J.C., and Bañó, M.C. (2017). Chimeric proteins tagged with specific 3xHA cassettes may present instability and functional problems. PLoS ONE *12*, e0183067.
47. Wang, Y., Shao, Q., Yu, X., Kong, W., Hildreth, J.E., and Liu, B. (2011). N-terminal hemagglutinin tag renders lysine-deficient APOBEC3G resistant to HIV-1 Vif-induced degradation by reduced polyubiquitination. J. Virol. *85*, 4510–4519.
48. Vecchio, L.M., Bermejo, M.K., Beerepoot, P., Ramsey, A.J., and Salahpour, A. (2014). N-terminal tagging of the dopamine transporter impairs protein expression and trafficking in vivo. Mol. Cell. Neurosci. *61*, 123–132.